Journal of Ultrafine Grained and Nanostructured Materials
https://jufgnsm.ut.ac.ir
Vol. 57, No.2, December 2024, pp. 128-134
Print ISSN: 2423-6845 Online ISSN: 2423-6837
DOI: 10.22059/jufgnsm.2024.02.03

Formation of nano-structured tribolayer on Ti-6Al-4V during sliding in a phosphate buffer saline solution

B. Rahmatian[a], H. M. Ghasemi [1, a], M. Heydarzadeh Sohi[a], P De Baets[b, c]

[a] School of Metallurgy and Materials Engineering, College of Engineering, University of Tehran, Tehran, Iran
[b] Ghent University, Department of Electromechanical, Systems and Metal Engineering, Soete Laboratory, Technologiepark 46, B-9052, Zwijnaarde, Ghent, Belgium
[c] Royal Institute of Technology, Unit of Systems and Component Design, Brinellvägen 83, 10044 Stockholm, Sweden

Recieved: 12 August 2024; Accepted: 4 October 2024

[1]Corresponding author, E-mail: hghasemi@ut.ac.ir

ABSTRACT

The formation of a tribological layer (i.e., tribolayer) affects friction and wear behavior during sliding. The mechanisms involved can be better understood by the characterization of this layer. The wear corrosion behavior of Ti-6Al-4V was studied using a reciprocating ball-on-flat tribometer at a frequency of 1 Hz and under normal loads of 1 N, 5 N, and 15 N against an alumina ball for 3600 cycles of sliding in a phosphate buffer saline (PBS) solution. Scanning Electron Microscopy (SEM) images, along with EDS analysis showed a greater coverage of a tribolayer under a normal load of 15 N. Transmission electron microscopy (TEM) studies indicated that a tribolayer with thickness up to 1000 nm, consisting of nanograins with diameters of less than 10 nm, formed on the deformed wear surface of Ti-6Al-4V under a normal load of 15 N. This protected tribolayer, under normal loads of 5 N and 15 N, resulted in a decrease of 40% in the coefficient of friction and a 15-20% reduction in the specific tribocorrosion rate compared with that at the lower applied load.

Keywords: *Ti-6Al-4V; Tribocorrosion; Biomaterials; Tribolayer, Nanostructured; TEM.*

1. Introduction

The wear process in a corrosive medium, known as tribocorrosion, often accelerates material removal, leading to a loss of the material functionality [1]. In human body joints, bio-tribocorrosion is a key mechanism that degrades metallic implants and reduces their lifespan [2]. Ti-6Al-4V is a commonly used metallic material in the biomedical field, particularly for joints application. Moreover, this alloy is being used in chemical processes as well as in the marine, aerospace, and automotive industries [3]. The passive film, formed under non-sliding conditions is easily disrupted by tribological action, resulting in direct contact between the tribopair [4]. The high adhesion between a titanium alloy and its mating surface is attributed to the alloy's high ductility and four free electrons in the valance band [5]. However, during sliding, a tribological layer can be formed on the material, altering its tribological properties.

For instance, Nedfors et al. reported [6] a reduction in the coefficient of friction due to the formation of B_2O_3/H_3BO_3 tribolayer on the wear surface of 316L stainless steel coated with NbB_{2-x} thin films. Additionally, Qi et al. [7] found that the thickness of the tribolayer on Ti-6Al-4V increased as the applied potential raised from 0.95 V to +0.5 V in a phosphate buffer saline (PBS) solution containing Bovine Serum Albumin (BSA). This

tribolayer protected the surface and reduced the material removal rate. Moreover, Yazdi et al. [8] showed that the formation of an oxygen diffusion layer (ODL) on Ti-6Al-4V through a thermal oxidation process led to a thicker tribofilm under high Hertzian contact stress in a PBS solution compared to the base material. They attributed the formation of the thick tribofilm to the lower plastic deformation in the ODL layer compared with Ti-6Al-4V during sliding.

Studies have shown that metallic implants can endure different stresses by changing the type of motions, such as walking, running, ascending or descending stairs, as well as the displacement of the implant itself [9,10]. Additionally, the formation and characteristics of tribofilms can be affected by numerous factors, including applied load, sliding speed, ambient solution, tribological pair, and sliding distance. This research paper investigated the effects of applied normal load (i.e., contact stress) on the tribological behavior of Ti-6Al-4V in a PBS solution. The objective of this work is to characterize the tribological layer formed on Ti-6Al-4V in a simulated body fluid using scanning and transmission electron microscopies (SEM & TEM) and to enhance the understanding of the correlation between the presence of tribolayer and tribocorrosion behavior of the alloy.

2. Experimental procedure

2.1. Materials

As-received Ti-6Al-4V plate was wire cut to obtain plane specimens with dimensions of 10 × 6 × 4 mm. The specimens were mechanically polished using SiC emery paper with 80 to 1000 grit sizes, and then ultrasonically cleaned with distilled water and acetone. An alumina ball with a diameter of 5 mm and hardness of 1670 HV was used as the mating surface.

2.2. Tribocorrosion tests

To simulate the sliding process in a hip joint, a reciprocating ball-on-flat tribometer with a stroke length of 6 mm was designed and built. Tribocorrosion tests were performed under normal loads of 1 N, 5 N, and 15 N against an alumina ball. These normal loads were selected to simulate various states of Hertzian contact pressures (730 up to 1800 MPa), which can occur in body joints [9]. The frequency of reciprocating motion was set to 1 Hz, resulting in a sliding speed of 12 mm/s. More details of the tribometer setup were reported in a previously published paper [11].

The tribocorrosion tests were conducted under open circuit potential (OCP), i.e., without imposing any potential, in a phosphate buffer saline (PBS) solution, which consisted of 8.0 g NaCl, 1.15 g Na_2HPO_4, 0.2 g KCl, and 0.2 g KH_2PO_4 dissolved in one liter of distilled water [12]. Prior to the sliding process, the tribopair remained in a PBS solution under the OCP condition for 15 minutes to achieve a steady state condition. The sliding process was performed for 1 h (i.e., 3600 cycles) and each test was repeated at least three times to ensure the repeatability of the results. Following each tribocorrosion test, the tribopair was ultrasonically cleaned for 6 minutes with distilled water.

2.3. Characterization

The worn area was measured at three different locations along the wear track using a contact profilometer (T-8000 HommelWerke). The average crosssectional worn area was multiplied by the stroke length of 6 mm to determine the volume of material removed due to the sliding process. To measure the microhardness of Ti-6Al-4V and wear surfaces, a load of 25 g was applied using a Vickers indenter for 10 s ($HV_{0.025}$), and an average of three measurements was reported. The wear surfaces were analyzed by a scanning electron microscope (FEI Model Quanta, FEG 450) equipped with energy-dispersive X-ray spectroscopy (EDS). A JEOL JEM2200FS transmission electron microscope (TEM) was used to characterize the tribolayer formed under a normal load of 15 N. The TEM sample was prepared as a crosssection of the wear track parallel to the sliding direction using a gallium focused-ion beam (FIB) (Dual Beam SEM, FEI Model Quanta-FEG 450). In this method, the focused beam was scanned across the wear surface to prepare a TEM electrontransparent film by removing a material above and below the region. This film contained the region of interest and was milled to a thickness of about 100 nm. A platinum layer was also deposited on the wear surface through a chemical vapor deposition (CVD) technique in the vacuum chamber of SEM to protect the initial surface atomic layers during the milling process. Bright-field transmission electron microscopy (BFTEM), scanning transmission electron microscopy with EDS elemental mapping, and selected area electron diffraction (SAED) patterns were utilized with an accelerated voltage of

200 kV. Notably, the SAED patterns were obtained using a SAD aperture with a diameter of 10 nm.

3. Results and discussion

3.1. Tribological behavior

Fig. 1 shows the tribocorrosion and specific tribocorrosion rates of Ti-6Al-4V under normal loads of 1 N, 5 N, and 15 N. According to Archard's wear law, the material removal rate (i.e., tribocorrosion rate) is directly proportional to the applied normal load [5]. As such, the specific tribocorrosion rate, which indicates the severity of the material removal rate at various loads, should be constant. However, this specific tribocorrosion rate decreased about 15-20% as the normal load was increased to 5 N and 15 N.

Fig. 2 depicts the variation of coefficient of friction (COF) over 3600 cycles of sliding of Ti6Al6V against an alumina ball under normal loads of 1 N and 15 N. The COF trend exhibited a lower amplitude of oscillation under the higher normal load of 15 N. Notably, the COF trend observed under a normal load of 5 N was similar to that at 15 N. The figure indicates that the mean coefficient of friction decreased by 40% from 0.55 to 0.33. The results could suggest a change

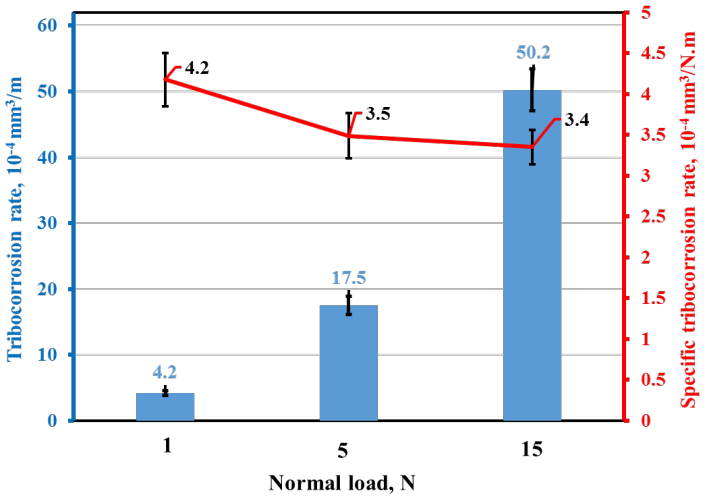

Fig. 1- Tribocorrosion and specific tribocorrosion rates of Ti-6Al-4V under normal loads of 1 N, 5 N, and 15 N.

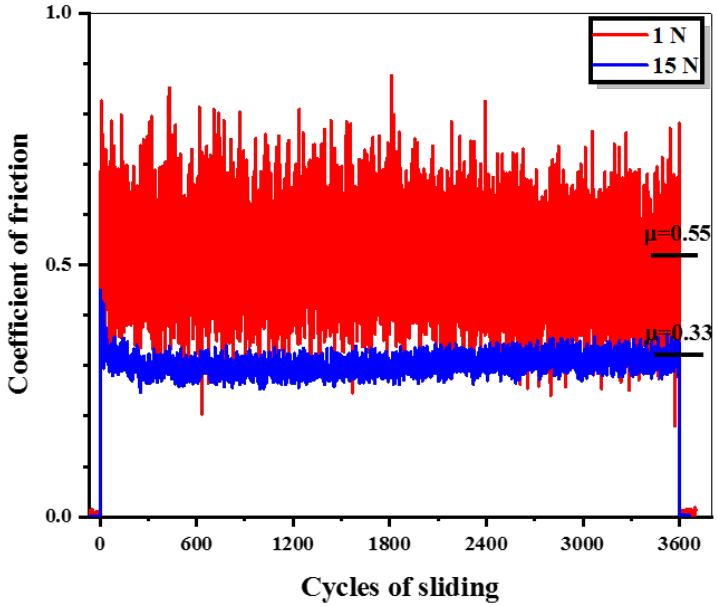

Fig. 2- Variation of coefficient of friction (μ) of Ti-6Al-4V sliding against alumina ball in PBS solution under normal loads of 1 N and 15 N.

in the nature of the interface, possibly due to the work-hardening effect and/or the presence of a tribological layer under the higher normal load.

To better illustrate the changes in the wear surface under various applied normal loads, backscattered and secondary SEM images of the wear surfaces of Ti-6Al-4V after 3600 cycles of sliding are shown in Figs. 3a-f. The backscattered electron images in Figs. 3a, c, and e reveal a higher coverage of darker patches (i.e., tribological layers) as the applied normal load was increased to 15 N. Table 1 presents the EDS analysis of the regions identified in Fig. 3. The presence of oxygen in the darker regions in Fig. 3e indicates that the tribolayers were oxidative in nature. During the sliding process, the surface temperature due to frictional heating can be estimated using Archard's surface temperature estimation [13]. The calculations indicate a surface temperature rise of only about 12 °C (i.e., a surface temperature of about 37 °C) when Ti-6Al-4V slides against an alumina ball under a normal load of 15 N at a frequency of 1 Hz. However, the sliding process may lower the activation energy required for the formation of chemical compounds.

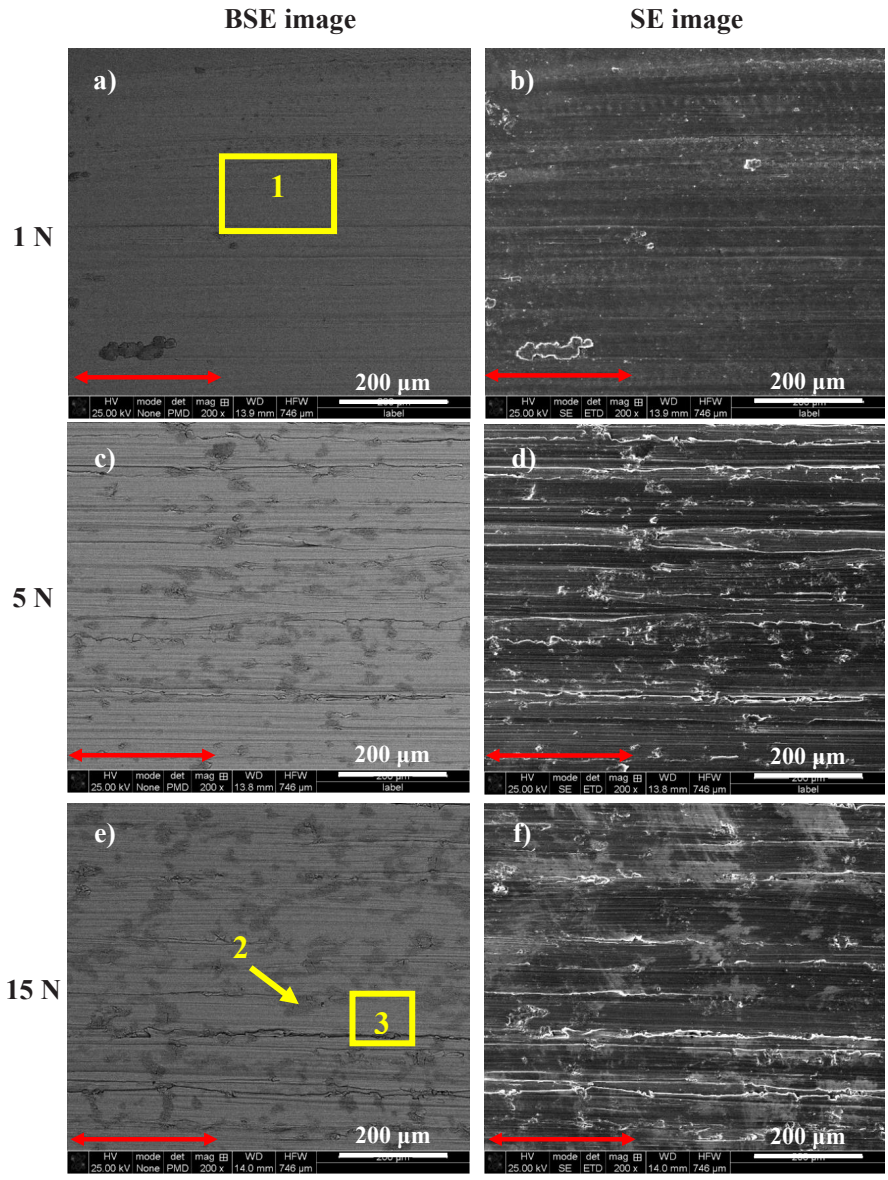

Fig. 3- SEM images of wear track of Ti-6Al-4V after 3600 cycles of sliding against alumina ball in PBS solution under normal loads of 1, 5, and 15 N. Two-headed arrows show the sliding direction.

Emission of exoelectrons (EEEs) released during tribomechanical and chemical action [14-17] could lead to the formation of oxide patches (i.e., tribolayer) on the sliding surface of Ti-6Al-4V, even at such a low temperature (Fig. 3). Moreover, the sliding process and mechanical perturbation can enhance the diffusion rates of ions by creating defects such as voids, dislocations, and vacancies, which contribute to the formation of the tribolayer on the wear surface [5].

The fluctuations in the coefficient of friction trend were due to the adhesion between Ti-6Al-4V and the alumina ball [18]. The presence of oxide patches (i.e., darker regions) reduced both adhesion and amplitude of friction oscillation between the mating surfaces. The oxide patches contributed to a reduction in adhesion between the mating surfaces. The oxide, due to a low shear strength and limited junction growth, reduced the coefficient of friction under applied normal loads of 5 N and 15 N.

Figs. 3b, d, and f indicate the formation of grooves on the wear surface of Ti-6Al-4V under normal loads of 1 N, 5 N, and 15 N. This is due to the low hardness (initially 325 HV) and high plastic deformation, which is originated from sufficient slip systems existed in Ti-6Al-4V alloy [18]. The presence of oxide patches and grooves suggests that plastic deformation and oxidative wear were the primary mechanisms under normal loads of 5 N and 15 N. However, the occurrence of ploughing in Fig. 1b indicates that the plastic deformation was the dominant wear mechanism at the lower normal load of 1 N.

After 3600 cycles of sliding under a normal load of 15 N, the plastic deformation resulted in approximately a 30% increase in hardness, from 325 HV on the undeformed Ti-6Al-4V substrate to about 425 HV on the wear surface. This increase in hardness was likely due to the formation of tribolayer and the work-hardening of Ti-6Al-4V during the sliding process [19]. The features of the tribolayer and sublayer will be discussed in the next section. Additionally, the higher coverage and durability of the tribolayer (i.e., oxide patches) on the wear surface under a normal load of 15 N resulted in a reduction of the specific tribocorrosion rate (i.e., Fig. 1b), the amplitude of oscillation in the coefficient of friction trend, and the mean coefficient of friction (Fig. 2).

3.2. Characterization of the Tribolayer

A TEM slice with a thickness of about 70 nm was extracted from the wear track of Ti-6Al-4V after 3600 cycles of sliding under a normal load of 15 N, using the focused ion beam (FIB) method. Fig. 4a shows a STEM image of the cross-sectional wear surface, which was obtained parallel to the sliding direction. The image reveals a tribolayer roughly 1000 nm thick on the wear surface. Figs. 4b and c show the EDS elemental maps for oxygen and titanium, respectively. The EDS maps indicate a high concentration of oxygen in the top tribolayer, confirming the corresponding EDS analyses presented in Table 1, derived from Fig. 3. This suggests that a much greater thickness of the tribolayer was formed during the sliding process, in

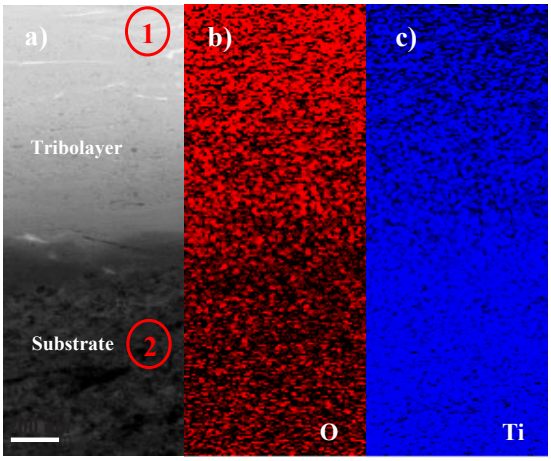

Fig. 4-a) STEM image of the prepared cross-section of wear track of Ti-6Al-4V after 3600 cycles of sliding against alumina ball in PBS solution under a normal load of 15 N; b) and c) corresponding EDS elemental maps of oxygen and titanium, respectively.

contrast to the 6 nm passive TiO_2 film on Ti-6Al-4V under non-sliding conditions reported in previous studies [20,21].

Figs. 5a and b show the SAED patterns of regions 1 and 2, as specified in Fig. 4a. Region 1 is located in the tribolayer about 100 nm from the wear surface, while region 2 is located in the substrate about 400 nm below the tribolayer. The SAD aperture with a diameter of 10 nm was used to obtain the SAED patterns. The continuous diffraction rings in Fig. 5a could suggest the formation of numerous nanograins, each less than 10 nm in diameter, within the tribolayer. Similarly, the ring patterns in the SAED pattern from region 2, beneath the tribolayer (Fig. 5b), could also indicate the presence of nanocrystalline grains in the Ti-6Al-4V subsurface. This suggested the development of a work-hardened layer during sliding, which enhanced the support of the tribolayer. The increased hardness of the wear surface compared to the base alloy (Ti-6Al-4V) was attributed to this work-hardened layer. The formation of ring patterns, along with the elongated diffraction spots, could be the result of a severe non-homogenous deformation in contact regions established during the sliding process [22].

The SAED patterns facilitate the identification of phases present in the material. The d-spacing, or interplanar distance, is inversely proportional to the distance between the diffracted spot and the central beam. Table 2 lists the d-spacing values obtained

Table 1- EDS analysis of regions specified in Fig. 3

Element (at. %)	Ti	Al	V	P	O
1	90.8	7.8	0.5	0.2	0.7
2	68.0	9.7	0.8	0.6	20.9
3	88.1	10.4	1.5	0.0	0.0

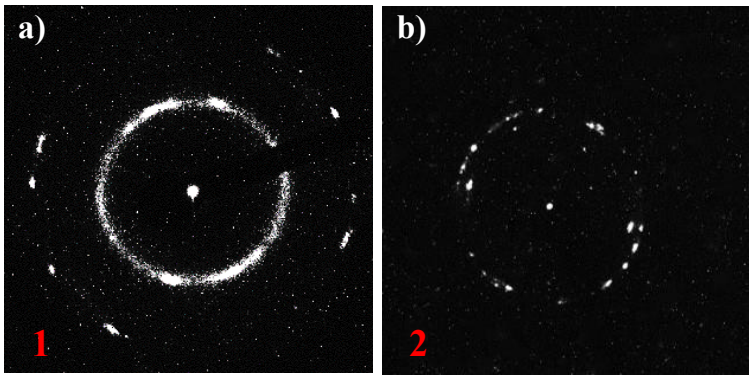

Fig. 5- SAED pattern of a) region 1, located in the tribolayer, 100 nm away from the wear surface, and b) region 2, about 400 nm below the tribolayer located in the deformed Ti-6Al-4V substrate indicated in Fig. 4.

Table 2- d spacing obtained according to the SAED pattern in Fig. 5a and corresponding Miller indices of the possible phases in the tribolayer compared with ICDD (International Centre for Diffraction Data)

	obtained d-spacing from SAED	Ti (α)	Ti (β)	TiO_2	Ti_2O_3
1st Ring	2.280	(1 0 1)	(1 1 0)	(2 0 0)	(1 1 3)
2nd Ring	1.355	(1 0 3)	(2 1 1)	(3 0 1)	(2 0 8)

from Fig. 5a, along with the corresponding Miller indices of the phases present in the tribolayer. Comparing these d-spacings with the miller indices obtained from the ICDD (i.e., International Center for Diffraction Data), suggested that the tribolayer consisted of TiO_2 (rutile), Ti_2O_3, αTi, and β-Ti phases.

4. Conclusions

This research paper investigates the tribological behavior of Ti-6Al-4V/alumina tribopair over 3600 cycles of reciprocating sliding in a PBS solution under normal loads of 1 N, 5 N, and 15 N. Additionally, the wear surfaces were analyzed by SEM and TEM. The following findings can be drawn from this study:

1. Increasing the applied load resulted in the formation of a tribolayer with greater coverage on the wear surface.
2. EDS analyses showed that the tribolayer formed during sliding in PBS solution was rich in oxygen.
3. The formation of the durable tribolayer significantly decreased the coefficient of friction and reduced the severity of the tribocorrosion process.
4. TEM study demonstrated that a tribolayer with a thickness of up to 1000 nm formed on the wear surface of Ti-6Al-4V under a normal load of 15 N.
5. The SAED patterns indicated that the sliding process induced the formation of two nanostructured layers with grains less than 10 nm: (1) tribolayer, and (2) deformed Ti-6Al-4V region beneath the tribolayer.

Acknowledgments

Dr. K.S. Pondicherry and Dr. V. Bliznuk from the Department of Electromechanical, Systems, and Metal Engineering at Ghent University are gratefully appreciated for their collaboration in performing TEM characterization.

References

1. Landolt D, Mischler S, Stemp M. Electrochemical methods in tribocorrosion: A critical appraisal. Electrochim Acta 2001;46:3913–29.
2. Cui WF, Niu FJ, Tan YL, Qin GW. Microstructure and tribocorrosion performance of nanocrystalline TiN graded coating on biomedical titanium alloy. Trans Nonferrous Met Soc China, English Ed 2019;29:1026–35.
3. Atar E, Kayali ES, Cimenoglu H. Characteristics and wear performance of borided Ti6Al4V alloy. Surf Coatings Technol 2008;202:4583–90.
4. Namus R, Nutter J, Qi J, Rainforth WM. Sliding speed influence on the tribo-corrosion behaviour of Ti6Al4V alloy in simulated body fluid. Tribol Int 2021;160:107023.
5. Hutchings I, Shipway P. Tribology: Friction and Wear of Engineering. Elsevier; London, 2017.
6. Nedfors N, Tengstrand O, Lu J, Eklund P, Persson POÅ, Hultman L, Jansson U. Superhard NbB2-x thin films deposited by dc magnetron sputtering. Surf Coatings Technol 2014;257:295–300.
7. Qi J, Guan D, Nutter J, Wang B, Rainforth WM. Insights into tribofilm formation on Ti-6V-4Al in a bioactive environment: Correlation between surface modification and micro-mechanical properties. Acta Biomater 2022;141:466–80.
8. Yazdi R, Ghasemi HM, Abedini M, Wang C, Neville A. Mechanism of tribofilm formation on Ti6Al4V oxygen diffusion layer in a simulated body fluid. J Mech Behav Biomed Mater 2018;77:660–70.
9. Liu F, Williams S, Fisher J. Effect of microseparation on contact mechanics in metal-on-metal hip replacements - A finite element analysis. J Biomed Mater Res - Part B Appl Biomater, 2015;103:1312–9.
10. Brand RA, Pedersen DR, Davy DT, Kotzar GM, Heiple KG, Goldberg VM. Comparison of Hip Force Calculations and Measurements in the Same Patient. The Journal of Arthroplasty, 1994;9:45-51.
11. Rahmatian B, Ghasemi HM, Heydarzadeh Sohi M, De Baets P. Tribocorrosion and corrosion behavior of double borided layers formed on Ti-6Al-4V alloy: An approach for applications to bio-implants. Corros Sci 2023;210:110824.
12. ASTM F2129–15, "Standard Test Method for Conducting Cyclic Potentiodynamic Polarization Measurements to Determine the Corrosion Susceptibility of Small Implant Devices", 2015.
13. Stachowiak G., Batchelor A. Engineering Tribology, Elsevier; London, 2013.
14. Yoshihiro Momose TN. Exoelectron emission from metals subjected to friction and wear, and its relationship to the adsorption of oxygen, water vapor, and some other gases. J Phys Chem, 1978;82:1509–15.
15. Czichos H. Tribology - A Systems Approach to the Science and Technology of Friction, Lubrication and Wear. vol. 1. Elsevier; Amsterdam, 1977.
16. Furey MJ, Ghasemi H, Tripathy BS, Kajdas C, Kempinski R, Hellgeth JW. Tribochemistry of the antiwear action of a dimer acid/glycol monoester on alumina. Tribol Trans 1994;37:67–74.
17. Ghasemi HM, Furey MJ, Kajdas C. Surface temperatures and fretting corrosion of steel under conditions of fretting contact. Wear 1993;162–164:357–69.
18. Yazdi R, Ghasemi HM, Abedini M, Monshi M. Interplay between mechanical wear and electrochemical corrosion during tribocorrosion of oxygen diffusion layer on Ti–6Al–4V in PBS solution. Appl Surf Sci 2020;518:146048.
19. Yazdi R, Ghasemi HM, Abedini M, Wang C, Neville A. Tribocorrosion behaviour of Ti6Al4V under various normal loads in phosphate buffered saline solution. Trans Nonferrous Met Soc China, English Ed 2020;30:1300–14.
20. Gai X, Bai Y, Li J, Li S, Hou W, Hao Y, et al. Electrochemical behaviour of passive film formed on the surface of Ti-6Al-4V alloys fabricated by electron beam melting. Corros Sci 2018;145:80–9.
21. Alves VA, Reis RQ, Santos ICB, Souza DG, de T, Pereira-da-Silva MA, et al. In situ impedance spectroscopy study of the electrochemical corrosion of Ti and Ti-6Al-4V in simulated body fluid at 25 °C and 37 °C. Corros Sci 2009;51:2473–82.
22. Johnson KL. Contact Mechanics. Cambridge University Press; Cambridge, 1987.